



HAL
open science

Gravitational phase transitions and instabilities of self-gravitating fermions in general relativity

Pierre-Henri Chavanis, Giuseppe Alberti

► **To cite this version:**

Pierre-Henri Chavanis, Giuseppe Alberti. Gravitational phase transitions and instabilities of self-gravitating fermions in general relativity. *Phys.Lett.B*, 2020, 801, pp.135155. 10.1016/j.physletb.2019.135155 . hal-02309051

HAL Id: hal-02309051

<https://hal.science/hal-02309051>

Submitted on 21 Jul 2022

HAL is a multi-disciplinary open access archive for the deposit and dissemination of scientific research documents, whether they are published or not. The documents may come from teaching and research institutions in France or abroad, or from public or private research centers.

L'archive ouverte pluridisciplinaire **HAL**, est destinée au dépôt et à la diffusion de documents scientifiques de niveau recherche, publiés ou non, émanant des établissements d'enseignement et de recherche français ou étrangers, des laboratoires publics ou privés.



Distributed under a Creative Commons Attribution - NonCommercial 4.0 International License

Gravitational phase transitions and instabilities of self-gravitating fermions in general relativity

Pierre-Henri Chavanis

Laboratoire de Physique Théorique, Université de Toulouse, CNRS, UPS, France

Giuseppe Alberti

*Laboratoire de Physique Théorique, Université de Toulouse, CNRS, UPS, France and
Living Systems Research, Roseggerstraße 27/2, A-9020 Klagenfurt am Wörthersee, Austria*

We discuss the occurrence of gravitational phase transitions and instabilities in a gas of self-gravitating fermions within the framework of general relativity. In the classical (nondegenerate) limit, the system undergoes a gravitational collapse at low energies $E < E_c$ and low temperatures $T < T_c$. This is called “gravothermal catastrophe” in the microcanonical ensemble and “isothermal collapse” in the canonical ensemble. When quantum mechanics is taken into account and when the particle number is below the Oppenheimer-Volkoff limit ($N < N_{OV}$), complete gravitational collapse is prevented by the Pauli exclusion principle. In that case, the Fermi gas undergoes a gravitational phase transition from a gaseous phase to a condensed phase. The condensed phase represents a compact object like a white dwarf, a neutron star, or a dark matter fermion ball. When $N > N_{OV}$, there can be a subsequent gravitational collapse below a lower critical energy $E < E_c''$ or a lower critical temperature $T < T_c'$ leading presumably to the formation of a black hole. The evolution of the system is different in the microcanonical and canonical ensembles. In the microcanonical ensemble, the system takes a “core-halo” structure. The core consists in a compact quantum object or a black hole while the hot halo is expelled at large distances. This is reminiscent of the red giant structure of low-mass stars or the implosion-explosion of massive stars (supernova). In the canonical ensemble, the system collapses as a whole towards a compact object or a black hole. This is reminiscent of the implosion of supermassive stars (hypernova).

PACS numbers: 04.40.Dg, 05.70.-a, 05.70.Fh, 95.30.Sf, 95.35.+d

I. INTRODUCTION

The study of phase transitions is an important problem in physics. Some examples include solid-liquid-gas phase transitions, superconducting and superfluid transitions, Bose-Einstein condensation, liquid-glass phase transition in polymers, liquid crystal phases, Kosterlitz-Thouless transition etc. Self-gravitating systems also undergo phase transitions but they are special because of the unshielded long-range attractive nature of the gravitational interaction [1–3]. This leads to unusual phenomena such as quasistationary states, negative specific heats, ensembles inequivalence, long-lived metastable states, and gravitational collapse. The statistical mechanics of systems with long-range interactions is also an important topic in statistical mechanics [4–6] because of its peculiarities and its various applications in astrophysics, plasma physics and hydrodynamics.

In this Letter, we consider the statistical mechanics of self-gravitating fermions in general relativity. This is a fundamental problem that combines general relativity, quantum mechanics and statistical mechanics. In addition, the thermodynamics of the self-gravitating Fermi gas can have application in relation to the physics of white dwarfs, neutron stars and dark matter halos made of massive neutrinos. It may also be related, as we shall see, to the supernova and hypernova phenomena. It represents therefore a topic of considerable interest both from a fundamental and an astrophysical point of view.

The statistical mechanics of self-gravitating systems dates back to the works of Antonov [7] and Lynden-Bell and Wood [8] who considered nonrelativistic classical stellar systems such as globular clusters. They enclosed the gas of stars within a spherical box of radius R in order to prevent its evaporation. They showed the absence of a statistical equilibrium state below a critical energy $E_c = -0.335GM^2/R$ in the microcanonical ensemble (MCE) or below a critical temperature $T_c = GMm/2.52k_B R$ in the canonical ensemble (CE) (the critical temperature T_c was found earlier by Emden [9]). In that case, the system collapses. The gravitational collapse in the MCE is called “gravothermal catastrophe” [8]. In the case of globular clusters, it leads ultimately to the formation of a binary star surrounded by a hot halo [10] (this structure has an infinite entropy $S \rightarrow +\infty$ at fixed energy [11]). The gravitational collapse in the CE is called “isothermal collapse” [12]. In the case of self-gravitating Brownian particles it leads to the formation of a Dirac peak containing all the mass [13] (this structure has an infinite free energy $F \rightarrow -\infty$ [11]).

We may expect that quantum mechanics will prevent complete gravitational collapse on account of the Pauli exclusion principle (for fermions) giving rise to an additional quantum pressure. This is indeed the case for a nonrelativistic system of self-gravitating fermions as shown by Fowler [14], Stoner [15] and Chandrasekhar [16] at $T = 0$ in the context of white dwarf stars. The statistical mechanics of self-gravitating fermions at finite

temperature in the nonrelativistic limit was developed by Hertel and Thirring [17], Baumgartner [18], Messer [19], Bilic and Viollier [20] and Chavanis [3, 21]. They showed that a gas of fermions experiences a gravitational phase transition from a gaseous phase to a condensed phase when the energy or the temperature passes below a critical value. In that case, an equilibrium state (gaseous or condensed) exists for all accessible values of temperature and energy. However, the situation is expected to change for the general relativistic Fermi gas because we already know from the work of Oppenheimer and Volkoff [22] on neutron stars that, at $T = 0$, there is no equilibrium state if the particle number N overcomes the Oppenheimer-Volkoff limit $N_{OV} = 0.39853 (\hbar c/G)^{3/2} m^{-3}$.¹

In this Letter, we report the results of our recent investigations concerning the statistical mechanics of self-gravitating fermions at finite temperature in the framework of general relativity. They complete the previous works of Bilic and Viollier [27, 28] and Roupas [29–31]. The complete study being extremely rich, all the details are given in a series of exhaustive papers [32–35]. These papers also contain a detailed history of the subject with a long list of references. In this Letter, we emphasize the main results of our study and refer to our companion papers for more details and additional results.

II. BASIC EQUATIONS

We consider a spherically symmetric self-gravitating system in general relativity described by a metric of the form $ds^2 = e^\nu c^2 dt^2 - r^2(d\theta^2 + \sin^2\theta d\phi^2) - e^\lambda dr^2$ where ν and λ are functions of r only. The statistical equilibrium state of the system is obtained by maximizing the entropy $S = -k_B \int C(f) e^{\lambda(r)/2} 4\pi r^2 dr d\mathbf{p}$ at fixed mass-energy $Mc^2 = \int f E(p) 4\pi r^2 dr d\mathbf{p}$ and particle number $N = \int f e^{\lambda(r)/2} 4\pi r^2 dr d\mathbf{p}$ [27, 29, 34]. Here $f(\mathbf{r}, \mathbf{p})$ is the distribution function (DF) and $e^{\lambda(r)/2} 4\pi r^2 dr$ is the proper volume element involving the metric coefficient $e^{\lambda(r)/2} = [1 - 2GM(r)/rc^2]^{-1/2}$ where $M(r)c^2$ is the mass-energy contained within the sphere of radius r . For fermions, S is the Fermi-Dirac entropy with $C(f) = f \ln(f/f_m) + (f_m - f) \ln(1 - f/f_m)$ where $f_m = 2/h^3$. In the nondegenerate (classical) limit $f \ll f_m$, the Fermi-Dirac entropy reduces to the Boltzmann entropy with $C(f) = f[\ln(f/f_m) - 1]$. The extremization problem leads to the Fermi-Dirac DF

$$f(\mathbf{r}, \mathbf{p}) = \frac{2}{h^3} \frac{1}{1 + e^{-\alpha} e^{E(p)/k_B T(r)}}, \quad (1)$$

where $E(p) = \sqrt{p^2 c^2 + m^2 c^4}$ is the energy of a particle and $T(r)$ is the local temperature. In general relativity,

the temperature is spatially inhomogeneous even at statistical equilibrium (Tolman's effect) [36]. The extremization of entropy at fixed mass-energy and particle number also yields the Tolman-Oppenheimer-Volkoff (TOV) equations [22, 36]

$$\frac{dM}{dr} = \frac{\epsilon}{c^2} 4\pi r^2, \quad (2)$$

$$\frac{1}{T} \frac{dT}{dr} = \frac{1}{\epsilon + P} \frac{dP}{dr} = -\frac{1}{c^2} \frac{\frac{GM(r)}{r^2} + \frac{4\pi G}{c^2} Pr}{1 - \frac{2GM(r)}{rc^2}}, \quad (3)$$

expressing the condition of hydrostatic equilibrium, and the Tolman-Klein [36, 37] relations $T(r) = T_\infty e^{-\nu(r)/2}$ and $\mu(r) = \mu_\infty e^{-\nu(r)/2}$ relating the local temperature $T(r)$ and the local chemical potential $\mu(r)$ to the metric coefficient $\nu(r)$ (T_∞ and μ_∞ are the temperature and the chemical potential measured by an observer at infinity). Their ratio $\alpha = \mu(r)/k_B T(r) = \mu_\infty/k_B T_\infty$ is constant since they are redshifted in the same manner. From the DF (1), we can express the particle number density $n(r) = \int f d\mathbf{p}$, the energy density $\epsilon(r) = \int f E d\mathbf{p}$ and the pressure $P(r) = (1/3) \int f p E'(p) d\mathbf{p}$ in terms of $T(r)$ and α . We can then obtain $T(r)$ by solving the TOV equations (2) and (3) with the boundary conditions $T(0) = T_0 \geq 0$ and $M(0) = 0$, and determining α by the constraint $N(R) = N$. The mass and the Tolman (global) temperature are then given by $M = M(R)$ and $T_\infty = T(R) \sqrt{1 - 2GM/Rc^2}$. Finally, we can plot the caloric curve $T_\infty(Mc^2)$ for a given value of N by varying T_0 from 0 to $+\infty$. Instead of the mass-energy Mc^2 it is better to use the binding energy $E = (M - Nm)c^2$ which reduces to the Newtonian energy $E = E_{\text{kin}} + W$ in the limit $c \rightarrow +\infty$. Finally, we introduce the dimensionless energy $\Lambda = -ER/GNm^2$ and the dimensionless inverse temperature $\eta = \beta_\infty GNm^2/R$ with $\beta_\infty = 1/k_B T_\infty$.

III. CLASSICAL SYSTEMS

The caloric curve $\eta(\Lambda)$ of a classical self-gravitating gas in general relativity depends on a single parameter $\nu = GNm/Rc^2$ called the compactness parameter. It is plotted in Fig. 1 for $\nu = 0.1$. It has the form of a double spiral parametrized by the energy density contrast $\mathcal{R} = \epsilon(0)/\epsilon(R)$ [30, 32]. The density contrast \mathcal{R} is minimum at the ‘‘center’’ of the caloric curve and increases along the series of equilibria in the directions of the spirals.

The cold spiral (on the right) is a relativistic generalization of the caloric curve obtained by Katz [38] for the nonrelativistic classical self-gravitating gas in Newtonian gravity. It corresponds to weakly relativistic configurations (except when ν is large). It exhibits a minimum energy in the MCE at E_c and a minimum temperature in the CE at T_c below which the system undergoes a gravitational collapse as in the nonrelativistic case. The hot spiral is a purely general relativistic result. It is similar (but not identical [35]) to the caloric curve obtained

¹ This is the general relativistic extension of the Anderson-Stoner-Chandrasekhar-Landau [23–26] maximum mass of special relativistic Newtonian white dwarf stars.

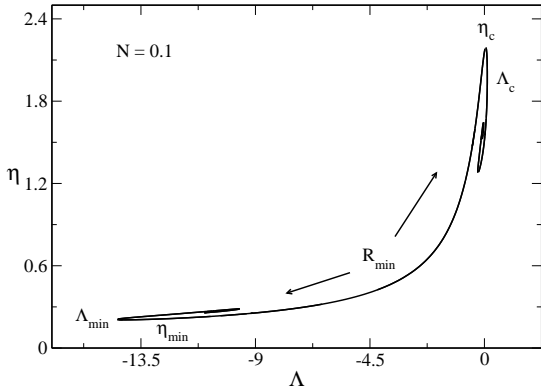


FIG. 1: Caloric curve of the general relativistic classical self-gravitating gas for $\nu = 0.1$. It presents a double spiral. The system collapses at low energies and low temperatures as in the case of a nonrelativistic classical self-gravitating gas in Newtonian gravity (cold spiral). It also collapses (towards a black hole) at high energies and high temperatures as in the case of the self-gravitating black-body radiation (hot spiral).

by Chavanis [39] for the self-gravitating black-body radiation. It corresponds to strongly relativistic configurations. It exhibits a maximum energy in the MCE at E_{\max} and a maximum temperature in the CE at T_{\max} above which the system undergoes a gravitational collapse leading presumably to the formation of a black hole.²

In the CE the series of equilibria is stable on the main branch between η_{\min} and η_c . According to the Poincaré criterion [38, 40], it becomes unstable at the first turning points of temperature η_{\min} and η_c where the specific heat is infinite passing from positive to negative values. A new mode of instability is lost at each subsequent turning point of temperature as the spirals rotate clockwise. In the MCE the series of equilibria is stable on the main branch between Λ_{\min} and Λ_c . According to the Poincaré criterion [38, 40], it becomes unstable at the first turning points of energy Λ_{\min} and Λ_c where the specific heat vanishes passing from negative to positive values.³ A new mode of instability is lost at each subsequent turning point of energy as the spirals rotate clockwise. There are two regions of ensembles inequivalence, one on each spiral, between the turning points of temperature and energy, i.e., in the first region of negative specific heat.

It has to be noted that the stable equilibrium states are in fact *metastable* as there is no global maximum of

entropy at fixed energy or global minimum of free energy for classical self-gravitating systems [7, 8]. However, these metastable states have a tremendously long lifetime, scaling as e^N , so they are stable in practice [41].⁴

The evolution of the caloric curve with ν is described in detail in [30, 32]. As ν increases, the cold and hot spirals approach each other, merge at $\nu'_S = 0.128$, form a loop above $\nu_S = 0.1415$, reduce to a point at $\nu_{\max} = 0.1764$, and finally disappear. The limit $\nu \rightarrow 0$ depends on the normalization that we use to plot the caloric curve. If we use the normalized variables $\Lambda = -ER/GN^2m^2$ and $\eta = \beta_{\infty}GNm^2/R$ appropriate to the nonrelativistic limit we find that the hot spiral is rejected at infinity and we obtain a limit curve corresponding to the caloric curve of the nonrelativistic classical self-gravitating gas. It has the form of a (cold) spiral with turning points at $\Lambda_c = 0.335$ and $\eta_c = 2.52$ [7–9, 38]. Alternatively, if we use the normalized variables $\mathcal{M} = GM/Rc^2$ and $\mathcal{B} = \beta_{\infty}Rc^4/GN$ appropriate to the ultrarelativistic limit we find that the cold spiral is rejected at infinity and we obtain a limit curve corresponding to the caloric curve of the ultrarelativistic classical self-gravitating gas [35]. It has the form of a (hot) spiral with turning points at $\mathcal{M}_{\max} = 0.24632$ (like for the self-gravitating black-body radiation [39, 42]) and $\mathcal{B}_{\min} = 17.809$ (different from the self-gravitating black-body radiation [35]).

Remark– Let us assume here that the previous results apply to star clusters (they may also apply to gaseous stars as discussed in Sec. V in which case the following discussion would be different). In Newtonian gravity, it can be shown that all the isotropic DFs of the form $f = f(\epsilon)$ with $f'(\epsilon) < 0$, where $\epsilon = v^2/2 + \Phi(r)$ is the energy of a star by unit of mass, are dynamically stable with respect to the Vlasov-Poisson equations (which describe collisionless stellar systems), even those that are thermodynamically unstable [43]. On the other hand, in general relativity, Ipser [44] has shown that dynamical stability with respect to the Vlasov-Einstein equations coincides with thermodynamical stability so that the equilibrium states located after the turning points of energy E_c and E_{\max} are both thermodynamically and dynamically unstable. To solve this apparent paradox, it is expected that the growth rate of the dynamical instability decreases as the relativity level decreases. From these considerations, one expects that the collapse at the turning point E_c of the cold spiral (weakly relativistic configurations) is mainly a thermodynamical – collisional – instability (gravothermal catastrophe) that takes place on a long, secular, timescale while the collapse at the turning point E_{\max} of the hot spiral (strongly relativistic configurations) is mainly a dynamical – collisionless – instability that takes place on a short, dynamical, timescale.

² Below T_c the system collapses because it is too cold and the thermal pressure cannot balance the gravitational attraction. By contrast, above E_{\max} the system collapses because it is too hot and feels “the weight of heat” [36] (energy is mass so that it gravitates).

³ Stable equilibrium states may have a negative specific heat in the MCE (isolated systems with fixed energy) while this is not possible in the CE (systems in contact with a heat bath with fixed temperature) [1–6].

⁴ Only a large random fluctuation can drive the system out of a local maximum of entropy (or local minimum of free energy). This is a rare event whose probability scales as e^{-N} . Accordingly, the time scale for this phenomenon is exponentially large.

IV. QUANTUM SYSTEMS

The caloric curve $T_\infty(E)$ of a quantum gas of fermions in general relativity depends on two parameters, the box radius R and the particle number N (throughout the paper, the radius is measured in terms of $R_* = (\hbar^3/m^4 Gc)^{1/2} = 0.11447 R_{OV}$ and the particle number is measured in terms of $N_* = (\hbar^3 c^3/m^6 G^3)^{1/2} = 2.5092 N_{OV}$) [33].

A. N -shape structure

We first consider a radius in the range $R_{CCP} = 12.0 < R < R_{MCP} = 92.0$ so that the caloric curve may display canonical, but not microcanonical, phase transitions [33].

For $N \ll N_{OV} = 0.39853$ we are in the nonrelativistic limit considered in [3, 17, 20, 21]. When $N < N_{CCP}(R)$, where $N_{CCP}(R) \simeq 2125/R^3$ corresponds to a canonical critical point, the caloric curve is monotonic like in Fig. 14 of [3] for $\mu = 10$ and there is no phase transition. When $N_{CCP}(R) < N < N_{OV}$ the caloric curve has an N -shape structure similar to Fig. 23 of [3]. In the MCE, the whole series of equilibria is stable. It displays a region of negative specific heat $C = dE/dT_\infty < 0$ between T_c and T_* . In the CE, the region of negative specific heat is replaced by a phase transition from the gaseous phase to the condensed phase. The condensed phase corresponds to a fermion ball at $T = 0$ (similar to a white dwarf or a neutron star) with only a tiny atmosphere. This structure has a very low energy. In principle, we expect a first order phase transition to take place at the transition temperature T_t at which the two phases have the same free energy.⁵ It would be marked by a discontinuity of energy. However, this first order phase transition does not take place in practice because the metastable gaseous states with $T_c < T < T_t$ (which are local but not global minima of free energy) have tremendously long lifetimes, scaling as e^N [41]. Not only they are stable in practice, but they are also more physical than strictly stable equilibrium states (global minima of free energy) which can be reached only if the system spontaneously crosses a huge barrier of free energy by forming a ‘‘critical droplet’’ (maximum of free energy) represented here by a fermion ball (quantum core), a very unlikely process (rare event) in the CE. As a result, the physical phase transition does not take place at T_t but rather at T_c (spinodal point), the temperature at which the metastable gaseous branch disappears. At that point, the system undergoes a gravitational collapse (isothermal collapse) and becomes denser and denser until quantum effects come into play and stabilize the system. Once in the condensed phase, if

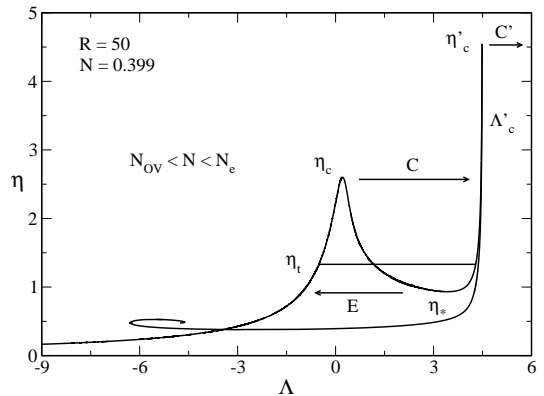


FIG. 2: Caloric curve for $N_{OV} < N \ll N_{max}$ (specifically $R = 50$ and $N = 0.399$). The arrows refer to the CE: (C) collapse at T_c from the gaseous phase to the condensed phase (fermion ball); (C') collapse at T'_c from the condensed phase (fermion ball) to a black hole; (E) explosion at T_* from the condensed phase (fermion ball) to the gaseous phase.

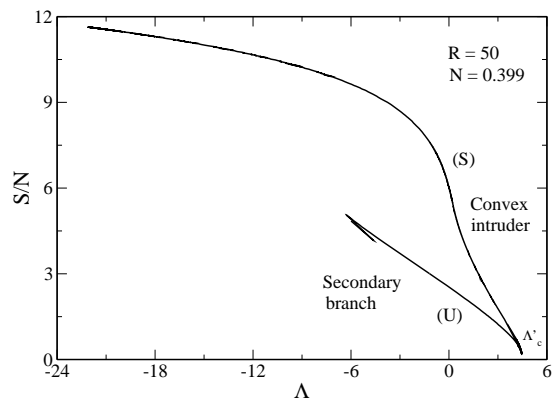


FIG. 3: Entropy per fermion as a function of the normalized energy for $N_{OV} < N \ll N_{max}$ (specifically $R = 50$ and $N = 0.399$). (S): stable; (U): unstable in the MCE.

the temperature increases, there is an explosion, reverse to the collapse, from the condensed phase to the gaseous phase at T_* (spinodal point). We can in this manner generate an hysteresis cycle in the CE [3].

When $N < N_{OV}$, there is an equilibrium state (gaseous or condensed) for any accessible value of energy $E \geq E_{min}$ or temperature $T \geq 0$. Quantum mechanics (Pauli’s exclusion principle) prevents gravitational collapse of classical self-gravitating systems below E_c or below T_c . However, as N approaches N_{OV} , general relativistic effects come into play. For $N_{OV} < N \ll N_{max}$, the caloric curve has the form of Fig. 2. In the MCE, there is no equilibrium state below a minimum energy E'_c . In that case the system is expected to collapse towards a black hole. The series of equilibria is stable until E'_c and becomes unstable afterwards. The entropy versus energy curve is plotted in Fig. 3. We can see the

⁵ The canonical transition temperature T_t can also be determined by a method analogous to that of Maxwell’s plateau in the discussion of the van der Waals gas.

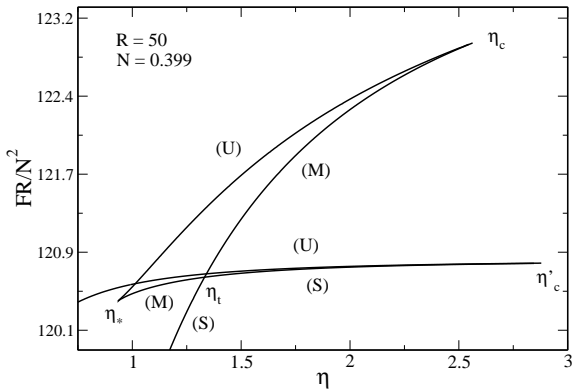


FIG. 4: Normalized free energy as a function of the normalized inverse temperature for $N_{\text{OV}} < N \ll N_{\text{max}}$ (specifically $R = 50$ and $N = 0.399$). (S): stable; (M): metastable; (U): unstable in the CE.

convex intruder $d^2S/dE^2 = d\beta_\infty/dE = -1/k_B T_\infty^2 C > 0$ associated with the region of negative specific heat on the caloric curve, the minimum energy E'_c at which the curve $S(E)$ presents a spike (because $\delta E = 0$ implies $\delta S = 0$ since $\delta S = \beta_\infty \delta E$), and the branch of unstable states with lower entropy than the stable states with the same energy. In the CE, the evolution is more interesting. As we reduce the temperature, starting from the gaseous phase, the system first undergoes a phase transition at T_c towards the condensed phase (fermion ball), followed by a catastrophic collapse at T'_c towards a black hole. The series of equilibria is stable until T_c , becomes unstable between T_c and T_* , is stable again between T_* and T'_c and becomes unstable again afterwards. The free energy versus temperature curve is plotted in Fig. 4. We can see the signal of a first order phase transition at T_t marked by the discontinuity of the first derivative $d(\beta_\infty F)/d\beta_\infty = E$ of the free energy (this first order phase transition does not take place in practice as we have explained) and the two spinodal points T_c and T_* at which the curve $F(T_\infty)$ presents a spike (because $\delta T_\infty = 0$ implies $\delta F = 0$ since $\delta(\beta_\infty F) = E\delta\beta_\infty$) and where zeroth order phase transitions (associated with the discontinuity of the free energy) take place. We also see the minimum temperature T'_c below which the system collapses towards a black hole (the curve $F(T_\infty)$ also presents a spike there). For large values of N , the caloric curve approaches the classical caloric curve of Fig. 1.

Remark – The equilibrium states in the region of negative specific heat have a core-halo structure with a quantum core (fermion ball) surrounded by an isothermal atmosphere. They are unstable in the CE (saddle points of free energy) and represent a “critical droplet” or a free energy “barrier” that the system must cross in order to trigger a phase transition from the gaseous phase to the condensed phase (a rare event as we have seen). By contrast, these core-halo solutions are stable in the MCE (maxima of entropy at fixed energy). They may

describe DM halos with a quantum core (representing a large bulge) and an isothermal atmosphere as suggested in [45, 46].

B. Z-shape structure

We now consider a radius in the range $R > R_{\text{MCP}} = 92.0$ so that the caloric curve may display both canonical and microcanonical phase transitions [33]. The description of the CE is the same as above so we focus on the MCE.

For $N \ll N_{\text{OV}}$ we are in the nonrelativistic limit considered in [3]. When $N < N_{\text{MCP}}(R)$, where $N_{\text{MCP}}(R) \simeq 2.20 \times 10^6/R^3$ corresponds to a microcanonical critical point, the situation is the same as above. When $N_{\text{MCP}}(R) < N < N_{\text{OV}}$ the caloric curve has a Z-shape structure similar to Fig. 15 of [3] (dinosaur’s neck). There is a phase transition from the gaseous phase to the condensed phase. The condensed phase corresponds to a fermion ball at $T = 0$ (similar to a white dwarf or a neutron star) surrounded by a hot and massive atmosphere.⁶ As before, the physical phase transition does not take place at the transition energy E_t where the two phases have the same entropy but rather at E_c (spinodal point), the energy at which the metastable gaseous branch disappears and the system collapses (gravothermal catastrophe). Once in the condensed phase, if the energy increases, there is an explosion, reverse to the collapse, from the condensed phase to the gaseous phase at E_* (spinodal point). We can in this manner generate an hysteresis cycle in the MCE [3].

For $N_{\text{OV}} < N \ll N_{\text{max}}$, the caloric curve has the form of Fig. 5. As we reduce the energy, starting from the gaseous phase, the system first undergoes a phase transition at E_c towards the condensed phase (fermion ball), followed by a catastrophic collapse at E'_c towards a black hole. The series of equilibria is stable until E_c , becomes unstable between E_c and E_* , is stable again between E_* and E'_c and becomes unstable again afterwards. The entropy versus energy curve is plotted in Fig. 6. We can see the signal of a first order phase transition at E_t marked by the discontinuity of the first derivative $dS/dE = \beta_\infty$ of the entropy (this first order phase transition does not take place in practice for the reason explained above) and the two spinodal points E_c and E_* , at which the curve $S(E)$ presents a spike and where zeroth order phase transitions (associated with the discontinuity of the entropy) take place. We also see the minimum energy E'_c be-

⁶ In the condensed phase the system has a core-halo structure. The core is condensed and behaves as a completely degenerate Fermi gas at $T = 0$ (because $k_B T \ll \mu(r)$). For physically relevant parameters we find that the condensed core contains about 1/4 of the total mass [33]. It has a very negative potential energy. Since the total energy is conserved the halo must have a very high kinetic energy, i.e., a very high temperature.

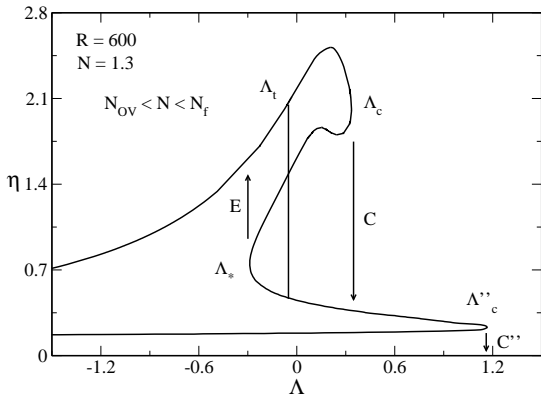


FIG. 5: Caloric curve for $N_{\text{OV}} < N \ll N_{\text{max}}$ (specifically $R = 600$ and $N = 1.3$). The arrows refer to the MCE: (C) collapse at E_c from the gaseous phase to the condensed phase (fermion ball); (C'') collapse at E''_c from the condensed phase (fermion ball) to a black hole; (E) explosion at E_* from the condensed phase (fermion ball) to the gaseous phase.

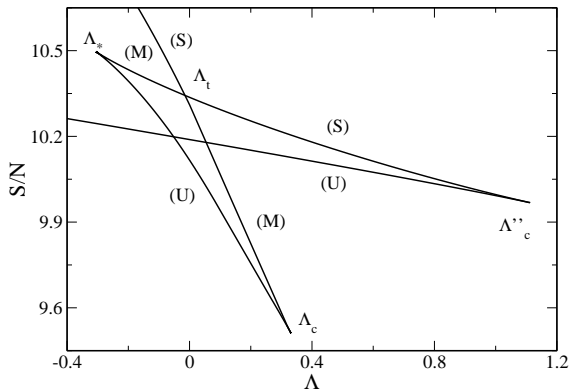


FIG. 6: Entropy per fermion as a function of the normalized energy for $N_{\text{OV}} < N \ll N_{\text{max}}$ (specifically $R = 600$ and $N = 1.3$). (S): stable; (M): metastable; (U): unstable in the MCE.

low which the system collapses towards a black hole (the curve $S(E)$ also presents a spike there). For large values of N , the caloric curve approaches the classical caloric curve of Fig. 1.

V. ASTROPHYSICAL APPLICATIONS

We can use our model to draw a physical scenario of stellar evolution (of course in a very simplified setting) complementing the results of [47, 48]. Let us consider a gaseous star initially with a high energy and a high temperature. We consider two types of evolution, a canonical one corresponding to Fig. 2 and a microcanonical one corresponding to Fig. 5. As the star radiates light into space, its temperature $T(t)$ (resp. energy $E(t)$) progressively decreases. As a result, the star follows the series

of equilibria on the gaseous branch until it reaches the minimum temperature T_c (resp. minimum energy E_c) at which point it becomes unstable and collapses. The collapse (due to a loss of hydrostatic equilibrium) continues until quantum mechanics comes into play. Then, if its mass is not too high, the star settles on a quiescent equilibrium state, a compact object similar to a white dwarf or a neutron star. The instability at the critical point corresponds to a saddle-center bifurcation. The evolution of the radius $R(t)$ of the star on the gaseous branch can be described by a Painlevé I equation of the form $\dot{R} = -ct - bR^2$ which explains the slow-fast transition in the life and death of a star [47, 48]. The following discussion depends whether we work in the CE or in the MCE.

In the CE it can be shown that the perturbation $\delta\rho(r)$ that triggers the instability at the critical temperature T_c has a core structure (one node) [12, 47] while the velocity perturbation $\delta v(r)$ has an implosive structure (no node) with $\delta v < 0$ (implosion) [47]. Therefore, the star is expected to collapse as a whole and form a compact object (white dwarf or neutron star) containing all the mass [3, 33, 47]. This phase transition is reminiscent of the hypernova phenomenon for supermassive stars (above $40 M_\odot$) which shows very intense and directive gamma ray bursts, but no explosion of matter (or a very faint one). When N is large enough ($N \gtrsim N_{\text{OV}}$) there is no equilibrium state anymore, and the star collapses towards a black hole.

In the MCE it can be shown that the perturbation $\delta\rho(r)$ that triggers the instability at the critical energy E_c has a core-halo structure (two nodes) [1, 48] while the velocity perturbation $\delta v(r)$ has an implosive-explosive structure (one node) with $\delta v < 0$ in the core (implosion) and $\delta v > 0$ in the halo (explosion) [48]. Therefore, the star is expected to split into a collapsing core, leading ultimately to a compact object (white dwarf or neutron star) containing a finite fraction ($\sim 1/4$) of the total initial mass [33], and an explosive (hot) halo expanding at large distances [3, 33, 48]. This phase transition is reminiscent of the red giant structure of stars with low or intermediate mass (roughly $0.3 - 8 M_\odot$) in a late phase of stellar evolution before the white dwarf stage. The implosion of the core and the explosion of the halo is also similar to the supernova explosion of massive stars with mass in the range of $8 - 40 M_\odot$ resulting in the formation of a neutron star. When N is large enough ($N \gtrsim 4N_{\text{OV}}$) there is no equilibrium state anymore, and the core collapses towards a black hole.

Similar results apply to stellar systems (globular clusters, galactic nuclei,...) and dark matter halos with, however, some differences. For these systems, only the MCE makes sense. At the critical energy E_c , they undergo the gravothermal catastrophe [8] and separate into a collapsing core and a halo. They are in hydrostatic equilibrium but their evolution is induced by the temperature gradient between the core and the halo and by the fact that the core has a negative specific heat $C_c < 0$

[8, 49]. Therefore, by losing heat, the core grows hotter, contracts, loses heat again to the profit of the halo, and evolves away from equilibrium in an unstoppable process (thermal runaway). In the case of classical objects like globular clusters, core collapse leads to a binary star surrounded by a hot halo [10]. In the case of fermionic dark matter halos where quantum mechanics becomes important at small scales, core collapse may lead to a “fermion ball” (representing a quantum core or a large bulge) + the expulsion of a hot envelope.⁷ The gravitational energy released by the collapse of the core heats up the envelope. In the box model, the atmosphere is held by the walls of the box. Without the box, the atmosphere is expelled at large distances (see Figs. 38 and 41 of [50] for an illustration in the context of the fermionic King model). Therefore, in the MCE the remnant is a fermion ball. Alternatively, in the case of galactic nuclei (star clusters) [51–53] and self-interacting dark matter [54] the collapsing core during the gravothermal catastrophe may become relativistic and finally experience a dynamical instability of general relativistic origin leading to a supermassive black hole of the right size ($10^6 \leq M/M_\odot \leq 10^9$) to explain quasars and active galactic nuclei (AGNs). In that case, the halo is not crucially affected by the collapse of the core and maintains its initial (isothermal) structure. The timescale governing the phase transition of these different systems (stars and stellar systems) is very different. For supernovae where the energy is carried quickly by neutrinos they are fast, a few days, but for globular clusters, galactic nuclei, and dark matter halos they are very slow (secular), of the order of the age of the Universe.

In summary, we suggest that the microcanonical phase transition occurring in the self-gravitating Fermi gas may be related to the onset of red giant structure or to the supernova phenomenon. In these spectacular events, the collapse of the core of the system (resulting ultimately in the formation of a white dwarf, a neutron star, or a black hole) is accompanied by the explosion and the expulsion of a hot envelope. Newtonian gravity is sufficient to describe the white dwarf and the planetary nebula that follow the red giant stage while general relativity is necessary to describe neutron stars or black holes formed from supernova explosion. Similarly, dark matter halos made of fermions may have a core-halo structure where the core may be a fermion ball (bulge) or a black hole depending on the mechanism at work.

Remark – It is interesting to compare our results with previous results obtained in the same context. Lynden-Bell and Wood [8], considering a classical self-gravitating gas in the MCE, found the emergence of a core-halo structure and related it to the onset of red giants. Hertel

and Thirring [17] argued that, through the electromagnetic radiation, a star is in heat contact with the rest of the Universe which acts as heat bath. As a result they worked in the CE and mentioned the analogy between the canonical phase transition and the formation of supernovae. However, this analogy may not be fully correct because the phase transition that they obtained just corresponds to an implosion. This is because they worked in the CE and considered relatively small systems while the phase transition leading to an implosion-explosion phenomenon, associated with a core-halo structure, occurs in the MCE for larger systems [33, 48]. Chandrasekhar, in the last sentence of [55], suggested that the supernova phenomenon may result from the inability of a star of mass greater than M_{Chandra} to settle down to the final state of complete degeneracy without getting rid of the excess mass. He assumed that sufficient mass is ejected so that the remnant has a mass $M_{\text{core}} < M_{\text{Chandra}}$. He did not anticipate the formation of a black hole when $M_{\text{core}} > M_{\text{Chandra}}$. At a qualitative level, our scenario encompasses and generalizes these original ideas.

VI. CONCLUSION

In this Letter, we have presented the main results of our recent investigations concerning the statistical mechanics of box-confined self-gravitating fermions at finite temperature in the framework of general relativity [32–35]. We have highlighted a situation of physical interest, namely the canonical and microcanonical phase transitions of self-gravitating fermions slightly above the OV limit. In that case, the system first displays a transition from a gaseous phase to a condensed phase (white dwarf, neutron star, fermion ball) followed by a gravitational collapse towards a black hole, as the temperature or the energy of the system is reduced. Our study completes the results of Bilic and Viollier [28] who studied the canonical phase transition of self-gravitating fermions below the OV limit. It also complements the study of Roupas [31] who considered self-gravitating fermions under different boundary conditions appropriate to neutron stars (by imposing a fixed density on the boundary of the system instead of a fixed size) and studied the stability of the system as a function of the temperature. Additional results and details of our study can be found in our companion papers [32–35]. In particular, we have obtained in Ref. [33] the complete phase diagram of the general relativistic Fermi gas in the (N, R) plane determining the canonical and microcanonical critical points of this system, thereby generalizing the Newtonian results of [3]. This phase diagram was useful, for example, to interpret the results of Roupas and Chavanis [56] who studied phase transitions in the general relativistic Fermi gas using different control parameters, GNm/Rc^2 and R/R_{OV} , instead of N/N_{OV} and R/R_{OV} .

We have also discussed astrophysical applications of our thermodynamical approach. In particular, we have

⁷ It is also possible that the halo is left undisturbed during the gravothermal catastrophe. In that case, the system acquires a core-halo structure with a quantum core (fermion ball) surrounded by an isothermal halo.

argued that the CE may be relevant to describe the life and death of supermassive stars which collapse (implode) without exploding (hypernova phenomenon) while the MCE may be relevant to describe the life and death of less massive stars which present a more complex evolution marked by the collapse (implosion) of the core and the

explosion of the halo (supernova phenomenon) [47, 48]. This is an interesting consequence of ensembles inequivalence for systems with long-range interactions [6]. Other interesting applications of the fermionic model in relation to dark matter halos made of massive neutrinos are given in [50, 57–59].

-
- [1] T. Padmanabhan, *Phys. Rep.* **188**, 285 (1990)
- [2] J. Katz, *Found. Phys.* **33**, 223 (2003)
- [3] P.H. Chavanis, *Int. J. Mod. Phys. B* **20**, 3113 (2006)
- [4] *Dynamics and thermodynamics of systems with long range interactions*, edited by T. Dauxois, S. Ruffo, E. Arimondo, M. Wilkens, *Lecture Notes in Physics* **602**, (Springer, 2002)
- [5] A. Campa, T. Dauxois, S. Ruffo, *Physics Reports* **480**, 57 (2009)
- [6] A. Campa, T. Dauxois, D. Fanelli, S. Ruffo, *Physics of long-range interacting systems* (Oxford University Press, 2014)
- [7] V.A. Antonov, *Vest. Leningr. Gos. Univ.* **7**, 135 (1962)
- [8] D. Lynden-Bell and R. Wood, *MNRAS* **138**, 495 (1968)
- [9] R. Emden, *Gaskugeln* (Leipzig, 1907)
- [10] S. Inagaki, D. Lynden-Bell, *Mon. Not. R. Astron. Soc.* **205**, 913 (1983)
- [11] C. Sire, P.H. Chavanis, *Phys. Rev. E* **66**, 046133 (2002)
- [12] P.H. Chavanis, *Astron. Astrophys.* **381**, 340 (2002)
- [13] C. Sire, P.H. Chavanis, *Phys. Rev. E* **69**, 066109 (2004)
- [14] R.H. Fowler, *MNRAS*, **87**, 114 (1926)
- [15] E.C. Stoner, *Phil. Mag.* **7**, 63 (1929)
- [16] S. Chandrasekhar, *Phil. Mag.* **11**, 592 (1931)
- [17] P. Hertel and W. Thirring, *Thermodynamic Instability of a System of Gravitating Fermions*. In: H.P. Dürr (Ed.): *Quanten und Felder* (Braunschweig: Vieweg 1971)
- [18] B. Baumgartner, *Commun. Math. Phys.* **48**, 207 (1976)
- [19] J. Messer, *J. Math. Phys.* **22**, 2910 (1981)
- [20] N. Bilic, R.D. Viollier, *Phys. Lett. B* **408**, 75 (1997)
- [21] P.H. Chavanis, *Phys. Rev. E* **65**, 056123 (2002)
- [22] J.R. Oppenheimer, G.M. Volkoff, *Phys. Rev.* **55**, 374 (1939)
- [23] W. Anderson, *Zeit. f. Phys.* **56**, 851 (1929)
- [24] E.C. Stoner, *Phil. Mag.* **9**, 944 (1930)
- [25] S. Chandrasekhar, *Astrophys. J.* **74**, 81 (1931)
- [26] L.D. Landau, *Phys. Zeit. Sow.* **1**, 285 (1932)
- [27] N. Bilic, R.D. Viollier, *Gen. Relat. Grav.* **31**, 1105 (1999)
- [28] N. Bilic, R.D. Viollier, *Eur. Phys. J. C* **11**, 173 (1999)
- [29] Z. Roupas, *Class. Quantum Grav.* **30**, 115018 (2013)
- [30] Z. Roupas, *Class. Quantum Grav.* **32**, 135023 (2015)
- [31] Z. Roupas, *Phys. Rev. D* **91**, 023001 (2015)
- [32] G. Alberti, P.H. Chavanis, [arXiv:1908.10316](https://arxiv.org/abs/1908.10316)
- [33] G. Alberti, P.H. Chavanis, [arXiv:1808.01007](https://arxiv.org/abs/1808.01007)
- [34] P.H. Chavanis, [arXiv:1908.10806](https://arxiv.org/abs/1908.10806)
- [35] P.H. Chavanis, [arXiv:1908.10817](https://arxiv.org/abs/1908.10817)
- [36] R.C. Tolman, *Phys. Rev.* **35**, 904 (1930)
- [37] O. Klein, *Rev. Mod. Phys.* **21**, 531 (1949)
- [38] J. Katz, *Mon. Not. R. Astron. Soc.* **183**, 765 (1978)
- [39] P.H. Chavanis, *Astron. Astrophys.* **483**, 673 (2008)
- [40] H. Poincaré, *Acta Math.* **7**, 259 (1885)
- [41] P.H. Chavanis, *Astron. Astrophys.* **432**, 117 (2005)
- [42] R.D. Sorkin, R.M. Wald, Z.Z. Jiu, *Gen. Relat. Grav.* **13**, 1127 (1981)
- [43] J.P. Doremus, M.R. Feix, G. Baumann, *Phys. Rev. Lett.* **26**, 725 (1971)
- [44] J.R. Ipser, *Astrophys. J.* **238**, 1101 (1980)
- [45] P.H. Chavanis, [Phys. Rev. D](https://arxiv.org/abs/1905.08137) **100**, 083022 (2019)
- [46] P.H. Chavanis, [arXiv:1905.08137](https://arxiv.org/abs/1905.08137)
- [47] Y. Pomeau, M. Le Berre, P.H. Chavanis and B. Denet, *Eur. Phys. J. E* **37**, 26 (2014)
- [48] P.H. Chavanis, Y. Pomeau, M. Le Berre and B. Denet, [arXiv:1307.4786](https://arxiv.org/abs/1307.4786) (in press)
- [49] W. Thirring, *Z. Physik* **235**, 339 (1970)
- [50] P.H. Chavanis, M. Lemou, F. Méhats, *Phys. Rev. D* **92**, 123527 (2015)
- [51] Y.B. Zel'dovich, M.A. Podurets, *Soviet Astron. – AJ* **9**, 742 (1966)
- [52] D. Fackerell, J. Ipser, K. Thorne, *Comments Ap. and Space Phys.* **1**, 134 (1969)
- [53] S.L. Shapiro, S.A. Teukolsky, *Phil. Trans. R. Soc. Lond. A* **340**, 365 (1992)
- [54] S. Balberg, S.L. Shapiro, S. Inagaki, *Astrophys. J.* **568**, 475 (2002)
- [55] M. Schönberg, S. Chandrasekhar, *Astrophys. J.* **96**, 161 (1942)
- [56] Z. Roupas, P.H. Chavanis, *Class. Quant. Grav.* **36**, 065001 (2019)
- [57] N. Bilic, G.B. Tupper, R.D. Viollier, *Lect. Notes Phys.* **616**, 24 (2003)
- [58] H.J. de Vega, P. Salucci, N.G. Sanchez, *Mon. Not. R. Astron. Soc.* **442**, 2717 (2014)
- [59] R. Ruffini, C.R. Argüelles, J.A. Rueda, *Mon. Not. R. Astron. Soc.* **451**, 622 (2015)